European Journal of Mechanics A/Solids 53 (2015) 10–18

Contents lists available at ScienceDirect

European Journal of Mechanics A/Solids

journal homepage: www.elsevier.com/locate/ejmsol

A continuum mechanical model for the description of solvent induced swelling in polymeric glasses: Thermomechanics coupled with diffusion

J. Wilmers [a], S. Bargmann [a, b, *]

[a] Institute of Materials Research, Materials Mechanics, Helmholtz-Zentrum Geesthacht, Germany
[b] Institute of Continuum and Material Mechanics, Hamburg University of Technology, Germany

ARTICLE INFO

Article history:
Received 8 August 2014
Accepted 13 March 2015
Available online 27 March 2015

Keywords:
Coupled problems
Polymeric glasses
Case II diffusion

ABSTRACT

The problem of interest is the numerical modelling of Case II diffusion in polymeric glasses. Case II diffusion is characterised by a strong coupling between diffusion and deformation and is highly temperature dependent. In this work, a general continuum mechanical framework describing a three-way coupling of thermomechanics and diffusion is adapted to the description of Case II diffusion.

Numerical studies are carried out to examine the capability of the model and the nature of the coupling. It is shown that the model is well suited for the description of solvent induced swelling as it predicts all characteristic properties of Case II diffusion.

1. Introduction

Understanding the mechanisms involved in diffusion of fluids in polymers is a field of great research interest, as the absorbed molecules may significantly alter the properties of the polymer matrix. The probably most common effect observed during fluid diffusion in polymers is swelling of the polymer. This swelling goes along with a change in the component's geometry and mechanical properties and might even lead to crazing or delamination in composites.

Classically, diffusion processes are described by Fick's laws. These, however, only describe the kinetics of an unhindered mass transport due to a concentration gradient. For the past centuries, it has become common knowledge that the diffusion behaviour in glassy polymers might strongly deviate from that predicted by Fick's laws. For most polymer-solvent systems, a variety of behaviours can be observed, depending on the solvent concentration or the temperature (Hopfenberg and Frisch, 1969).

These differences in behaviour are the result of molecular interactions between the polymer and the solvent which might cause a delay in the diffusion kinetics or plasticisation of the polymer.

The range of possible anomalous diffusion behaviours is limited on one side by Fickian (Case I) diffusion and on the other side by Case II diffusion as defined by Alfrey et al. (1966). Case II behaviour is characterized by the occurrence of several phenomena:

1. A sharp front forms between the plasticised and the dry region of the polymer.
2. Behind the front, a constant concentration as well as an equilibrium state of swelling are achieved. The swelling remains even after desorption.
3. The front moves with constant velocity, independent of time and concentration. In combination with 2., this translates to mass uptake kinetics that are linear in time.
4. Ahead of the front, a Fickian precursor of varying size occurs. This is due to the small amount of solvent that diffuses within the free volume of the polymeric glass.
5. The desorption process follows Fickian diffusion kinetics.

None of these characteristics alone are conclusive for the identification of Case II behaviour, as they might occur during other types of anomalous diffusion as well.

These characteristics are not described by the classical Fickian relations, and, consequently, there are a number of modelling approaches aiming to describe different aspects of non-Fickian diffusion. As the mechanism of Case II diffusion is not fully understood, different models apply different fundamental principles

* Corresponding author. Institute of Materials Research, Materials Mechanics, Helmholtz-Zentrum Geesthacht, Germany.
E-mail address: swantje.bargmann@tuhh.de (S. Bargmann).

http://dx.doi.org/10.1016/j.euromechsol.2015.03.002

and assumptions. The earliest models focus on the influence of the deformation on the flux relationship, e.g., Durning and Tabor (1986). More recently, models for the diffusion flux that consider the reproduction of the characteristic kinetics have been proposed, e.g., in Gallyamov (2013), where a dual-mode sorption approach is used to account for front formation without plasticisation, or the quasi-hyperbolic diffusion law for Case II in Wilmers and Bargmann (2014). For a more detailed overview of models describing anomalous and Case II diffusion kinetics, we refer to De Kee et al. (2005), Bargmann et al. (2011) and references therein.

A thorough model of Case II diffusion, however, has to account for the characteristic transport kinetics as well as the strong coupling of concentration and deformation that is responsible for the swelling. Furthermore, it is well known that the diffusion behaviour in polymers strongly depends on temperature (Duda et al., 1982) as do the plasticisation and the mechanical properties of the polymer.

For polymeric solids, a coupling of diffusion and deformation is often encountered in practical applications, not only in the limit of Case II diffusion. There exists a number of models describing the relationship between solvent concentration and deformation in hydrogels, investigating both, the influence of stresses on the diffusion behaviour (Derrien and Gilormini, 2006) and the diffusion-induced swelling (Baek and Srinivasa, 2004; Hong et al., 2008; Bouklas and Huang, 2012; Wang and Hong, 2012). These coupled models are derived from thermodynamic considerations and can be applied to the description of typical phenomena known from hydrogel processing, e.g., buckling of thin films (Liu et al., 2012).

However, classical Fickian diffusion occurs in hydrogels and not all of the choices in the description of the mechanical behaviour in hydrogel models are also valid for the polymeric glasses which exhibit Case II diffusion.

In Govindjee and Simo (1993), a continuum mechanical framework is proposed explicitly for Case II diffusion, coupling concentration and displacement. This framework has been implemented for numerical studies in Vijalapura and Govindjee (2003, 2005) with great rigour but with restriction to the quasi-static case.

All of these models consider only the coupling between diffusion and deformation and neglect the strong temperature dependence. In McBride et al. (2011a, 2011b), Steinmann et al. (2012), the framework proposed in Govindjee and Simo (1993) is coupled to thermomechanics without specification of the constitutive relations or the form of the free energies. Based on the general set of equations presented in McBride et al. (2011a), the current work proposes a numerical model for Case II diffusion. Formulations for the diffusion flux law and the free energy of mixing are presented that capture the distinct diffusion kinetics and swelling behaviour of Case II. This specialised model is implemented into a finite element code to examine the capabilities of the chosen formulation.

2. Theory

The modelling approach follows the continuum mechanical framework for Case II diffusion which was proposed in Govindjee and Simo (1993) and has been extended to the thermomechanically coupled case in McBride et al. (2011a). This approach does not differentiate between the solvent and the polymer but describes the mixture as a continuum.

In the first part of this Section, the derivation of the governing equations is outlined. For further details regarding this derivation, the reader is referred to Govindjee and Simo (1993), McBride et al. (2011a, 2011b). In Section 2.2, the constitutive equations that describe the distinct Case II behaviour are established.

2.1. Governing equations

As is customary in non-linear continuum mechanics, it is differentiated between the reference and the current configuration, cf. Fig. 1. The motion $\boldsymbol{\varphi}$ maps the reference configuration $\mathscr{B}_0$ to the current configuration according to $\mathscr{B} = \boldsymbol{\varphi}(\mathscr{B}_0(\boldsymbol{X}, t))$. With that the deformation gradient $\boldsymbol{F}$ is defined by

$$\boldsymbol{F}(\boldsymbol{X}, t) := \nabla \boldsymbol{\varphi}(\boldsymbol{X}, t), \tag{1}$$

where ∇ denotes the gradient in space with respect to the reference configuration. Within this setup, the governing equations describing Case II diffusion are derived from fundamental balance equations.

2.1.1. Conservation of mass

In the reference setting $\mathscr{B}_0$, a continuum body has the mass density ρ_0, while in the current configuration ,$\mathscr{B}$ the density is ρ. Here and in the following, mass density refers to mass per volume of the whole mixture, i.e., a value that can be obtained from straightforward experiments.

The conservation of the solid mass m, i.e., the mass of the polymer, is

$$\frac{\mathrm{d}}{\mathrm{d}t} \int_{\mathscr{B}} \mathrm{d}m = \frac{\mathrm{d}}{\mathrm{d}t} \int_{\mathscr{B}} \rho \, \mathrm{d}v = 0 \tag{2}$$

which, following standard arguments, gives

$$\rho_0 = J\rho \quad \text{with } J = \det \boldsymbol{F}. \tag{3}$$

Here, det denotes the determinant operator.

For the diffusing species, the balance of mass is formulated by consideration of the concentration c, which is defined as the mass of solvent per volume of the mixture.

$$\frac{\mathrm{d}}{\mathrm{d}t} \int_{\mathscr{B}} c \, \mathrm{d}v = - \int_{\partial\mathscr{B}} \boldsymbol{j} \cdot \boldsymbol{n} \, \mathrm{d}a + \int_{\mathscr{B}} w \, \mathrm{d}v, \tag{4}$$

where $\boldsymbol{j}$ denotes the diffusion flux over the boundary $\partial\mathscr{B}$ and ω the internal sources of solvent molecules. The negative sign appears because the surface normal vector $\boldsymbol{n}$ is positive in the outward direction.

This expression is pulled back to the reference configuration as

$$\frac{\mathrm{d}}{\mathrm{d}t} \int_{\mathscr{B}_0} \underbrace{cJ}_{c_0} \, \mathrm{d}V = - \int_{\partial\mathscr{B}_0} \underbrace{\left[J\boldsymbol{j} \cdot \boldsymbol{F}^{-T}\right]}_{\boldsymbol{J}} \cdot \boldsymbol{N} \, \mathrm{d}A + \int_{\mathscr{B}_0} \underbrace{wJ}_{W} \, \mathrm{d}V. \tag{5}$$

The fact that $\mathscr{B}_0$ is constant allows to interchange the succession of time derivation and integration. Application of the divergence theorem and localisation then gives

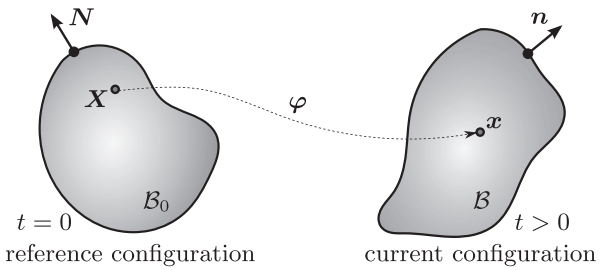

Fig. 1. Schematic representation of the relationship between reference and current configuration. A continuum body occupying the reference configuration $\mathscr{B}_0$ is mapped to the current configuration $\mathscr{B}$ by the motion $\boldsymbol{\varphi}$.

$$\dot{c}_0 = -\mathrm{Div}\boldsymbol{J} + W, \tag{6}$$

where the superscript dot denotes the time derivative and Div is the divergence operator with respect to the reference configuration.

2.1.2. Balance of linear and angular momentum

Following standard arguments, cf., e.g., Holzapfel (2000), the local form of the balance of linear momentum is formulated as

$$\rho_0 \ddot{\boldsymbol{x}} = \mathrm{Div}\boldsymbol{P} + \rho_0 \boldsymbol{b}, \tag{7}$$

where $\boldsymbol{P}$ denotes the first Piola-Kirchhoff stress tensor relating momentary forces to the reference area. The vector $\boldsymbol{b}$ is the body force density.

Evaluation of the balance of angular momentum shows that the second Piola-Kirchhoff stress tensor $\boldsymbol{S}$ defined by $\boldsymbol{S} = \boldsymbol{F}^{-1}\cdot\boldsymbol{P}$ is symmetric. Therefore, $\boldsymbol{P}\cdot\boldsymbol{F}^T = \boldsymbol{F}\cdot\boldsymbol{P}^T$.

2.1.3. Balance of internal energy

The first law of thermodynamics postulates the conservation of energy. For the description of a diffusion process, one has to take into account that the diffusing solvent contributes to the internal energy ε of the mixture.

To this end, an equation of state for the chemical potential of the mixture is assumed:

$$\mu_s = \varphi_s - \theta\eta_s. \tag{8}$$

Here, θ is the absolute temperature and φ_s and η_s denote the specific enthalpy and specific entropy contributed to the system by mixing. Only the enthalpic part of the chemical potential contributes to the change in the total internal energy, while the entropic part appears in the balance of entropy. As they are introduced to the system via solvent uptake, these contributions are directly related to the solvent flux over the boundary.

With that, the local balance of internal energy is given by

$$\rho_0\dot{\varepsilon} = \boldsymbol{P}:\dot{\boldsymbol{F}} - \mathrm{Div}\left(\underbrace{\boldsymbol{Q} + \varphi_s\boldsymbol{J}}_{\boldsymbol{Q}_{\mathrm{eff}}}\right) + \underbrace{\rho_0 r + \varphi_s W}_{Q_{\mathrm{eff}}}. \tag{9}$$

In the following, the contributions of the heat flux $\boldsymbol{Q}$ and the diffusion flux $\boldsymbol{J}$ are condensed to the coupled effective value $\boldsymbol{Q}_{\mathrm{eff}}$. Analogously, the change in internal energy caused by the sources of heat and diffusing species within the body, $\rho_0 r$ and φW, are condensed to Q_{eff}.

2.1.4. Balance of entropy

The balance of entropy with respect to the reference configuration reads

$$\rho_0\dot{\eta} = -\mathrm{Div}\left(\frac{\boldsymbol{Q}}{\theta} + \eta_s\boldsymbol{J}\right) + \frac{\rho_0 r}{\theta} + \eta_s W + \frac{1}{\theta}\Gamma_0, \tag{10}$$

where $\Gamma_0 \geq 0$ is the dissipation density.

Applying standard arguments and assuming a specific Helmholtz free energy of the form $\psi = \varepsilon - \theta\eta$ gives the balance of entropy in its Clausius–Duhem form. With the equation of state for the chemical potential Eq. (8) and introducing the coupled effective term $\boldsymbol{H}_{\mathrm{eff}} := \frac{1}{\theta}\boldsymbol{Q} + \eta_s\boldsymbol{J}$ this formulation reduces to

$$\boldsymbol{P}:\dot{\boldsymbol{F}} - \rho_0\dot{\psi} - \rho_0\eta\dot{\theta} - \boldsymbol{H}_{\mathrm{eff}}\cdot\nabla\theta - \boldsymbol{J}\cdot\nabla\mu_s + \mu_s\dot{c}_0 \geq 0. \tag{11}$$

The Helmholtz energy is chosen to be of the general form $\psi = \psi(\boldsymbol{C}, c_0, \theta, \boldsymbol{\Xi}; \boldsymbol{X})$. Here, $\boldsymbol{\Xi}$ denotes the set of internal variables.

To obtain the constitutive relations, the balance of entropy (11) is examined using the standard Coleman–Noll procedure, yielding

$$\boldsymbol{P} = 2\rho_0\boldsymbol{F}\cdot\frac{\partial\psi}{\partial\boldsymbol{C}}, \quad \mu_s = \rho_0\frac{\partial\psi}{\partial c_0}, \quad \eta = -\frac{\partial\psi}{\partial\theta}, \tag{12}$$

and the reduced dissipation inequality

$$-\boldsymbol{J}\cdot\nabla\mu_s - \boldsymbol{H}_{\mathrm{eff}}\cdot\nabla\theta - \rho_0\frac{\partial\psi}{\partial\boldsymbol{\Xi}}\cdot\dot{\boldsymbol{\Xi}} \geq 0, \tag{13}$$

which is to be satisfied by the constitutive equations.

2.1.5. Temperature evolution

The evolution equation for the temperature is derived from the energy balance in its localised form Eq. (9), and the constitutive relations for the entropy density given in Eq. (12). Combining these equations gives the following relation for the temperature evolution

$$\begin{aligned} -\rho_0\theta\frac{\partial^2\psi}{\partial\theta^2}\dot{\theta} = {} & -\boldsymbol{J}\cdot\nabla\mu_s - \mathrm{Div}\left(\theta\boldsymbol{H}_{\mathrm{eff}}\right) + \theta H_{\mathrm{eff}} - \rho_0\frac{\partial\psi}{\partial\boldsymbol{\Xi}}\cdot\dot{\boldsymbol{\Xi}} \\ & + \theta\frac{\partial}{\partial\theta}\left[\boldsymbol{P}:\dot{\boldsymbol{F}} + \mu_s\dot{c}_0 + \rho_0\frac{\partial\psi}{\partial\boldsymbol{\Xi}}\cdot\dot{\boldsymbol{\Xi}}\right] \end{aligned} \tag{14}$$

with $H_{\mathrm{eff}} := \frac{\rho_0 r}{\theta} + \eta_s W$. The specific heat capacity of the material is defined by $C_p := -\theta\frac{\partial^2\psi}{\partial\theta^2}$.

In Eq. (14), the coupled nature of the proposed framework is particularly distinct: The coupling between temperature evolution and deformation which gives rise to the effect of structural heating is incorporated through the thermal derivative of the stress power $\boldsymbol{P}:\dot{\boldsymbol{F}}$, while the effective entropy fluxes and sources, $\boldsymbol{H}_{\mathrm{eff}}$ and H_{eff}, include both thermal and diffusional contributions.

2.2. Material model

The framework presented in Section 2.1 describes a general system in which diffusion, heat conduction and deformation are coupled. In the following, the Helmholtz energy and the laws of diffusion and heat conduction necessary to apply the general framework to Case II diffusion are formulated. Special attention is paid to deriving the free energy of mixing which is responsible for the coupling between diffusion and deformation. Furthermore, a new diffusion law accounting for Case II kinetics is introduced to the model.

2.2.1. Helmholtz energy

Following Govindjee and Simo (1993), the Helmholtz free energy is assumed to be additively decomposed into

$$\psi = \psi^{\mathrm{eq}}(\boldsymbol{C}, \theta) + \psi^{\mathrm{neq}}(\boldsymbol{C}, \theta, \boldsymbol{\Xi}) + \psi^{\mathrm{mix}}(\boldsymbol{C}, c_0, \theta), \tag{15}$$

where ψ^{eq} is the free energy of an elastic material, ψ^{neq} accounts for non-equilibrium contributions and ψ^{mix} is the free energy of mixing.

To describe the equilibrium thermomechanical material behaviour of the polymer, a Neo-Hookean material model is chosen:

$$\begin{aligned} \rho_0\psi^{\mathrm{eq}} = {} & \frac{\mu}{2}[\boldsymbol{C} - \boldsymbol{I}]:\boldsymbol{I} + \frac{\lambda}{2}\ln^2 J - \mu\ln J \\ & + \rho_0 C_p\left[\theta - \theta_0 - \theta\ln\frac{\theta}{\theta_0}\right] \\ & - 3\alpha\left[\lambda + \frac{2}{3}\mu\right][\theta - \theta_0]\frac{\ln J}{J}, \end{aligned} \tag{16}$$

with the Lamé constants μ and λ, the thermal expansion coefficient α and the reference temperature θ_0.

In accordance with Govindjee and Simo (1993), the non-equilibrium contribution of the material behaviour is described by

$$\frac{\partial \psi^{\mathrm{neq}}}{\partial \boldsymbol{C}} = \int_{-\infty}^{t} \beta \exp\left(-\frac{t-s}{\tau_{\mathrm{relax}}(s)}\right) \frac{\mathrm{d}}{\mathrm{d}s}\left[\frac{\partial \psi^{\mathrm{eq}}}{\partial \boldsymbol{C}}(s)\right] \mathrm{d}s. \tag{17}$$

Here, β is a dimensionless parameter describing the ratio of Young's moduli in the glassy and the rubbery state and τ_{relax} is the visco-elastic relaxation time of the polymer.

To determine the functional relation of the mixing contribution ψ^{mix}, the Flory–Huggins theory of polymer mixtures, cf., e.g., Flory (1970), Fried (2003), is applied. The Flory–Huggins model describes the mixing of a low-molecular-weight solvent and polymer on the basis of a theoretical lattice, as shown schematically in Fig. 2. One lattice site in this model can only be occupied by a single molecule. To account for the large difference in size and molecular weights between the solvent and the polymer, the polymer is represented by a chain of molecular segments, each occupying one lattice site. These segments are chosen so that the volume occupied by a chain segment is approximately equal to that occupied by a solvent molecule.

In this framework, the entropy of mixing is obtained via statistical considerations following the Boltzmann relation, which relates the change in entropy to the number of possible arrangements of N_p polymer molecules and N_s solvent molecules in the lattice. From that, the specific entropy of mixing is given by (see (Flory, 1942))

$$\Delta S^{\mathrm{mix}} = -\frac{k_B}{rN_p m_p}\left[N_s \ln\frac{N_s}{N_s + rN_p} + N_p \ln\frac{rN_p}{N_s + rN_p}\right]. \tag{18}$$

Here, N_p and N_s denote the number of polymer and solvent molecules, respectively. Furthermore, r is the number of chain segments per polymer molecule (i.e., for most systems approximately the degree of polymerisation), and m_p is the mass of a chain segment, with k_B the Boltzmann constant.

As m_p gives the mass of a polymer chain segment, m_s is the mass of a single solvent molecule. With that, the concentration and the density can be written as

$$c_0 = \frac{N_s m_s}{V} \quad \text{and} \quad \rho_0 = \frac{rN_p m_p}{V}.$$

Using these relations, Eq. (18) is rearranged to

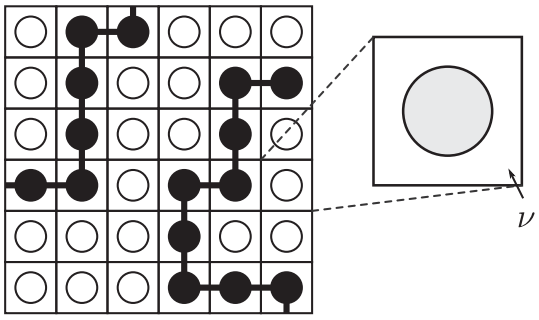

Fig. 2. Two-dimensional depiction of Flory–Huggins model lattice. Every lattice side is occupied by either a solvent molecule (open circle) or a segment of the polymer chain (filled circle).

$$\Delta S^{\mathrm{mix}} = -\frac{k_B}{\rho_0}\left[\frac{c_0}{m_s}\ln\left(\frac{c_0}{c_0 + \rho_0\frac{m_s}{m_p}}\right) + \frac{\rho_0}{rm_p}\ln\left(\frac{\rho_0}{c_0\frac{m_p}{m_s} + \rho_0}\right)\right]. \tag{19}$$

The enthalpy of mixing is given in the framework of the Flory–Huggins model by consideration of the interaction between neighbouring molecules. The change in energy if a solvent-polymer contact is formed is given by

$$\Delta\omega_{ps} = \omega_{ps} - 0.5\left[\omega_{ss} + \omega_{pp}\right], \tag{20}$$

where ω_{ij} is the energy of a contact i–j. The number of contacts of polymer and solvent is approximately equal to the number of possible contacts of a solvent molecule (i.e., the coordination number z of the lattice), times the probability that the site in question is occupied by a polymer chain segment. This probability is equal to the volume fraction of polymer in the current volume. Therefore, the specific mixing enthalpy is given by

$$\Delta H^{\mathrm{mix}} = \frac{1}{\rho_0 V} z N_s \frac{rN_p\nu}{\nu}\Delta\omega_{ps}. \tag{21}$$

Here, ν denotes the volume of a lattice site. As the reference volume V is the volume of the unswollen polymer, the relation $V = rN_p\nu$ holds. With this relation and the identity $\nu = JV$, the probability term is $\frac{rN_p\nu}{\nu} = \frac{1}{J}$. Furthermore, the dimensionless Flory–Huggins interaction parameter $\chi := \frac{z\Delta\omega_{ps}}{k_B\theta}$ is introduced. Thus, Eq. (21) becomes

$$\Delta H^{\mathrm{mix}} = \frac{1}{\rho_0} k_B\theta\chi \frac{c_0}{m_s}\frac{1}{J}. \tag{22}$$

The Gibbs potential of the mixing is given by $\Delta G^{\mathrm{mix}} = \Delta H^{\mathrm{mix}} - \theta\Delta S^{\mathrm{mix}}$.

From the equation of state, Eq. (8), it is evident that the chemical potential is a Gibbs potential. As it accounts for the change in Gibbs free enthalpy if an infinitesimal amount of the solvent is added to the system, μ_s is determined from the above relations by

$$\mu_s = \frac{\partial \Delta G^{\mathrm{mix}}}{\partial N_s} = \frac{\partial \Delta H^{\mathrm{mix}}}{\partial N_s} - \theta\frac{\partial \Delta S^{\mathrm{mix}}}{\partial N_s}. \tag{23}$$

The specific enthalpy and entropy of the solvent as introduced in Eq. (8) can thus be determined by $\varphi_s = \frac{\partial \Delta H^{\mathrm{mix}}}{\partial N_s}$ and $\eta_s = \frac{\partial \Delta S^{\mathrm{mix}}}{\partial N_s}$, respectively, cf. Appendix A.1.

Evaluating the balance of entropy by the Coleman–Noll procedure yields

$$\mu_s = \rho_0\frac{\partial \psi}{\partial c_0} = \rho_0\frac{\partial \psi^{\mathrm{mix}}}{\partial c_0}. \tag{24}$$

The mixing contribution to the Helmholtz potential can therefore be derived by integration of the chemical potential which yields

$$\psi^{\mathrm{mix}} = \frac{k_B\theta}{\rho_0^2 V}\left[c_0\chi\frac{1}{J} + c_0\ln\left(\frac{c_0}{c_0 + \rho_0\frac{m_s}{m_p}}\right) + \rho_0\frac{m_s}{rm_p}\ln\left(\frac{c_0 + \rho_0\frac{m_s}{m_p}}{\rho_0\frac{m_s}{m_p}}\right)\right] + \gamma, \tag{25}$$

As the chemical potential is a Gibbs potential, the concentration-independent value γ accounts for the difference between the Gibbs

and the Helmholtz free energy per amount of solvent. This relates to a change in pressure and temperature upon mixing. At constant pressure, this change is negligible (Mark and Erman, 2007), thus, in the following we assume γ=0.

2.2.2. Diffusion and heat conduction

Case II diffusion kinetics cannot be described by Fick's law. The behaviour is characterised by a wave-like solvent propagation with a constant diffusion front. To account for this non-classical behaviour, a new diffusion law has been introduced in Wilmers and Bargmann (2014). The derivation is based on a dual-phase-lag extension of Fick's first law

$$\boldsymbol{J}(\boldsymbol{X}, t+\tau_j) = -\boldsymbol{D}(c_0, \theta, J)\cdot\nabla c_0(\boldsymbol{X}, t+\tau_c), \tag{26}$$

where τ_j and τ_c denote retardation times, representing the delay in formation of the concentration gradient and the flux due to molecular interactions. This expression for the diffusion flux, however, does not necessarily guarantee that the dissipation inequality is fulfilled. To ascertain that the model produces thermodynamically sound results, the fulfilment of the dissipation inequality is checked for every quadrature point during calculation, cf. A.2.

The coupling of the diffusion behaviour to temperature and deformation is accounted for by the diffusion coefficient as a function of concentration, temperature and the determinant of the deformation gradient given by

$$\boldsymbol{D}(c_0, \theta, J) = \boldsymbol{D}_0[1-\phi_s]^2[1-2\chi\phi_s]\exp\left(-\frac{E_A}{R\theta} + \delta\left[\frac{c_0}{c_{\text{eq}}} - 0.5\right]\right), \tag{27}$$

where the volume fraction of the solvent is given by $\phi_s = \frac{v_s}{v} = \frac{c_0}{J\rho_s}$. Equation (27) is a combination of different well known dependencies. The temperature dependence of the solvent's self diffusion coefficient is known to follow an Arrhenius relation with the activation energy E_A, cf. e.g. Duda et al. (1982). Furthermore, the exponential dependence on the concentration with a constant factor δ is valid for a number of Case II systems (Wu and Peppas, 1993) and is responsible for the formation of the sharp front in the model, see Wilmers and Bargmann (2014) for further details. The multiplicator involving the solvent volume fraction φ_s generalizes this relation to the mutual diffusion coefficient (Duda et al., 1982). These dependences of the diffusion coefficient will be maintained in the following. For better readability, however, they are not stated explicitly anymore.

Combining the first order Taylor expansion with respect to time of Eq. (26) with the mass balance of the diffusing species, Eq. (6), under the assumption that no solvent molecules are created or destroyed within the polymer gives the following quasi-hyperbolic diffusion law

$$\dot{c}_0 + \tau_j\ddot{c}_0 = \text{Div}(\boldsymbol{D}\cdot\nabla c_0) + \tau_c\text{Div}(\boldsymbol{D}\cdot\nabla\dot{c}_0). \tag{28}$$

This diffusion law allows to describe the characteristic wave-like propagation and exhibits a constant front velocity, as shown in Wilmers and Bargmann (2014).

The heat conduction in amorphous polymers follows Fourier's law

$$\boldsymbol{Q} = -\boldsymbol{K}\cdot\nabla\theta, \tag{29}$$

with $\boldsymbol{K}$ denoting the material's heat conductivity.

3. Numerical examples

The equations established in the previous section are solved using a finite element discretisation in space. In time, an implicit Euler scheme is applied. This system is implemented in a C++ code utilising the program library deal.II (Bangerth et al., 2007).

The primary fields, i.e., the concentration, the displacement and the temperature, are approximated using linear functions. To interpolate the spatial gradient of the chemical potential μ_s occurring in the temperature evolution equation (14) and the dissipation inequality (13), a fourth equation is introduced to be fulfilled on element nodes, relating the specific enthalpy of mixing φ_s to the primary fields according to

$$\varphi_s = \frac{k_B\theta}{\rho_0 V}\frac{\chi}{J}, \tag{30}$$

see Appendix A.1.

In the numerical examples, the diffusion of toluene in polystyrene is examined, which has been shown to exhibit Case II kinetics for small toluene concentrations (Gall and Kramer, 1991). Furthermore, this system is a common example in experimental studies and, thus, material constants and characteristic values are readily available. The material parameters used in this contribution are given in Table 1.

The two-way coupling between diffusion and deformation in Case II diffusion arises from the plasticisation of the material by the absorbed solvent. Ahead of the diffusion front, where almost no solvent exists, the polymer remains in its rigid, glassy state. The mixture behind the front, however, is plasticised and, thus, has a different mechanical behaviour – including different Lamé parameters.

In Table 1 the Lamé constants for the glassy and the plasticised state are given. For concentrations greater than 0.5 c_{eq}, i.e., ahead of the front, the values for the plasticised state are used. This relates to a decrease in Young's modulus to approximately 1/20-th of the glassy value. The Poisson's ratio remains constant. A further temperature dependence of the mechanical properties is neglected as the plasticisation is in the focus of the examination.

Besides this change in the mechanical behaviour of the material, the coupling is introduced to the system via the dependence of the diffusion coefficient on the volume fraction of the solvent according to Eq. (27) and the Helmholtz free energy of mixing, cf. Eq. (25).

For the numerical examples, a cuboidal geometry as shown in Fig. 3 is examined. The geometry is discretised using linear hexahedral elements. To accurately capture the sharp diffusion front, the mesh is finer in x-direction, resulting in a discretisation with 2214 degrees of freedom. As the propagation velocity increases with temperature, the timestep size is reduced for higher applied temperatures, thus, ranging from 0.2 min to 12.5 min.

The displacement of the cuboid is constrained on three adjacent faces, for each in the plane's normal direction. Additionally, Dirichlet boundary conditions for the concentration and temperature are applied on only the small one of these three faces. The boundary conditions for concentration and temperature are chosen to be the equilibrium concentration c_{eq} and a constant temperature above the reference temperature $\theta_0 = 293.15$ K, respectively. For all surfaces, the concentration and temperature fluxes are assumed to vanish.

3.1. Case II diffusion

This setup and an imposed heating to 333.15 K (89.3% of the polymer's glass transition temperature) on the small face are used

Table 1
Material parameters for polystyrene and toluene.

	Symbol	Value	Source
Equilibrium concentration	c_{eq}	0.13 g/cm^3	Gall and Kramer (1991)
Maximum diffusion coefficient	D_0	$4.50714 \cdot 10^8$ cm^2/min	Gall and Kramer (1991)
Activation energy	E_A	1.13 eV	Gall and Kramer (1991)
Variation parameter of concentration dependence	δ	5	Wilmers and Bargmann (2014)
Flory interaction parameter	χ	0.133	Schuld and Wolf (1999)
Retardation time (flux)	τ_j	6732.45 min	[a]
Retardation time (gradient)	τ_c	50 min	
Mass density of the polymer	ρ_0	1.04 g/cm^3	Delassus and Whiteman (1999)
Mass density of the solvent	ρ_s	0.8669 g/cm^3	
Number of polymer segments	r	3500	Gall and Kramer (1991)
Mass polymer chain segment	m_p	$1.73 \cdot 10^{-25}$ kg	
Mass solvent molecule	m_s	$1.53 \cdot 10^{-25}$ kg	
Lamé constants (glassy)	λ	2.8 GPa	
	μ	1.2 GPa	
Lamé constants (plasticised)	λ	0.14 GPa	
	μ	0.06 GPa	
Viscoelastic relaxation time	τ_{relax}	$5 \cdot 10^3$ min	Govindjee and Simo (1993)
Specific heat capacity	C_p	1250 J/(kg K)	
Thermal expansion coefficient	α	$9.0 \cdot 10^{-5}$ 1/K	Delassus and Whiteman (1999)
Heat conductivity	K	0.17 W/(m K)	

[a] Estimated from velocity values given in Gall and Kramer (1991) using the Deborah number theory (Vrentas et al., 1975).

to investigate the model's capability to describe Case II behaviour. The results are presented in Figs. 4–7.

Fig. 4 displays the deformation and solvent transport over time. The sharp Case II front is upheld over the whole diffusion time. Behind the front, concentration and swelling are in equilibrium.

Fig. 5 shows the concentration, temperature and stress fields in the swollen geometry after an exposure of 200 min. Behind the solvent front, the polymer swells considerably while almost no deformation besides thermal expansion occurs in the low-concentration region. In the temperature field, a heating of a few millikelvin is visible. This is the effect of the heat of mixing as introduced via the chemical potential into the temperature evolution equation (14), cf. also Fig. 7.

The distinct deformation behaviour results in the occurrence of stresses in the sample. Directly ahead of the front where the polymer is still glassy and unable to deform, tensile stresses arise. In the layer behind the front, the material is subjected to compressive strains because the swelling is restricted by the adjacent glassy region.

This behaviour is further illustrated in Fig. 6 depicting the Cauchy stress distribution and the step-like concentration profiles in the unconstrained edge of the cuboid for different time steps. The stresses visible at a position of $x = 0$ μm arise from the displacement constraints on the yz-plane.

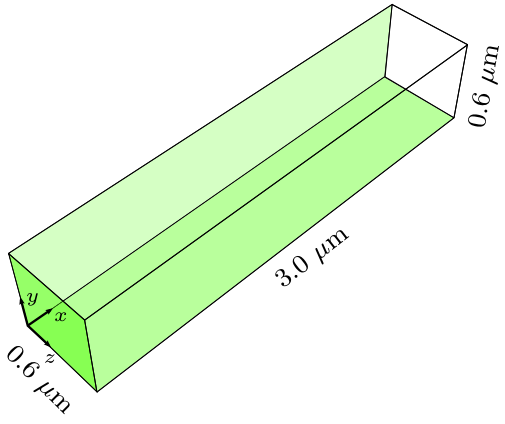

Fig. 3. Geometry of the sample. On the coloured surfaces, Dirichlet boundary conditions are applied. The other surfaces are traction free and diffusion or heat fluxes vanish.

In Fig. 7, the temperature profile over the undeformed specimen at different temperatures is depicted. For Case II diffusion, heat conduction is orders of magnitude faster than the solvent transport. For this reason, the heating of one face leads to a homogeneous temperature of θ=333.15 K in the whole specimen almost immediately. Further changes in the temperature are caused by two opposing effects, namely the thermoelastic behaviour of the material and the induced heat of mixing. In the beginning, the swelling of the polymer causes structural cooling, which is captured by the term describing the change of the stress power with temperature in Eq. (14). Over time, as the solvent concentration increases, the influence of the heat of mixing on the temperature evolution exceeds that of the stress power, causing a heating of the material. Fig. 7 shows that the maximum of the temperature profile occurs just at the diffusion front.

3.2. Investigation of the coupling

As the previous section has demonstrated the capability of the proposed model to fully predict the characteristic properties of Case II diffusion, a further investigation of the effects of coupling diffusion, deformation and temperature is carried out.

To investigate the influence the temperature has on the diffusion kinetics and the swelling, further simulations have been carried out using the same setup as introduced in Fig. 3 with different applied temperatures.

In Fig. 8, concentration profiles for different applied temperatures are depicted. As the temperature in the material increases, the front velocity increases as well, following an Arrhenius relation as is typical for Case II diffusion as a thermally activated process (Lasky et al., 1988; Gall and Kramer, 1991).

Furthermore, for higher temperatures, the solvent front widens because the diffusivity in the glassy region increases according to the temperature dependence of the diffusion coefficient visible in Eq. (27). With this rise in the diffusivity, the Fickian precursor becomes less pronounced. For the low temperature profiles, the Fickian precursor as the small region ahead of the front with a low solvent concentration is clearly visible. A higher diffusivity in the glassy region means that more solvent diffuses further into the

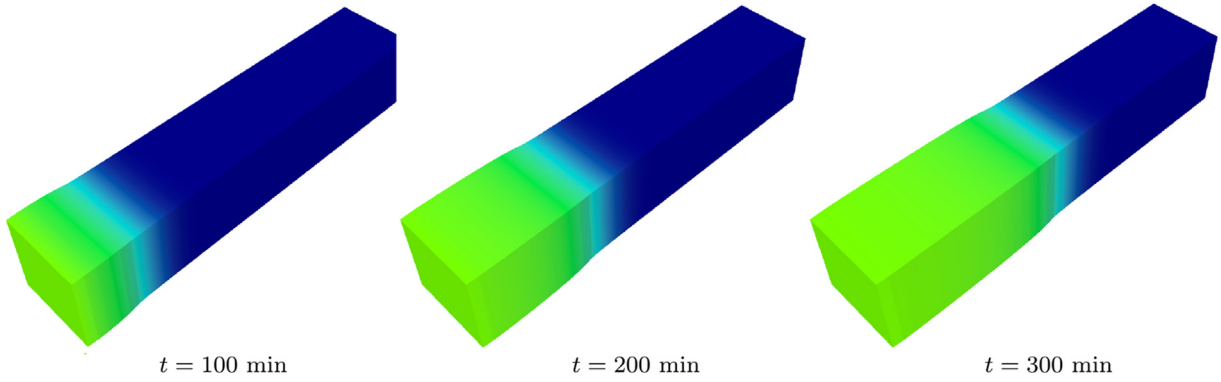

Fig. 4. Temporal evolution of Case II diffusion. A sharp concentration front moves with constant velocity through the specimen. Behind the front, a constant concentration and an equilibrium state of swelling are established. The severe swelling due to solvent uptake is clearly visible.

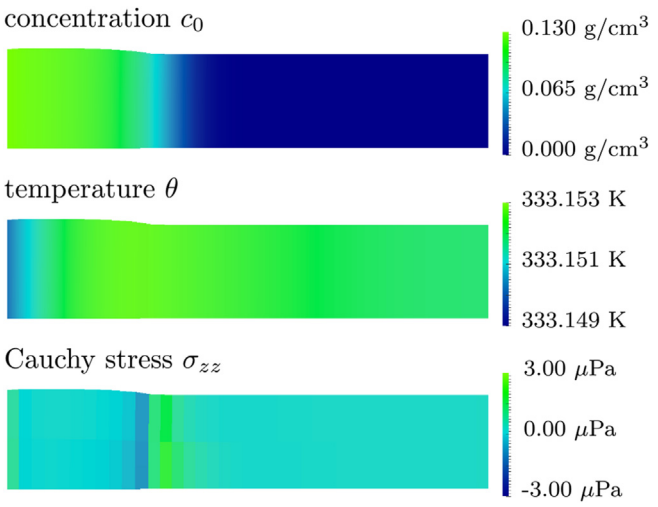

Fig. 5. Distribution of concentration c, temperature θ and the Cauchy stress component σ_{zz} in the swollen sample after an exposure time of 200 min.

glassy region, thus, the Fickian precursor widens as well. The broadening of the Fickian precursor and the front indicates how the diffusion behaviour transitions from Case II to Fickian at temperatures above the glass transition.

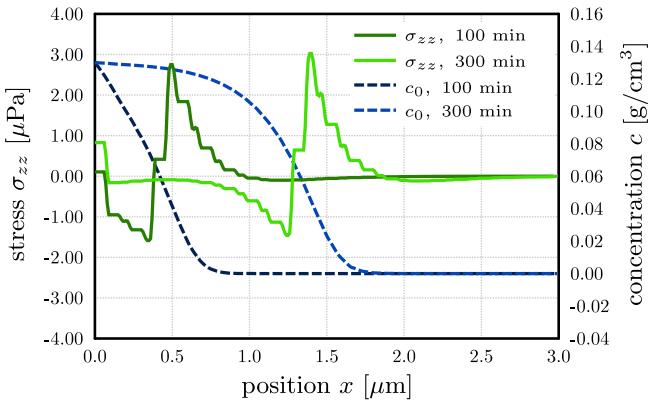

Fig. 6. Cauchy stress and concentration profiles in x-direction of the undeformed sample at different exposure times. At the concentration front, a jump in the stresses occurs because only the plasticised, high-concentration region swells.

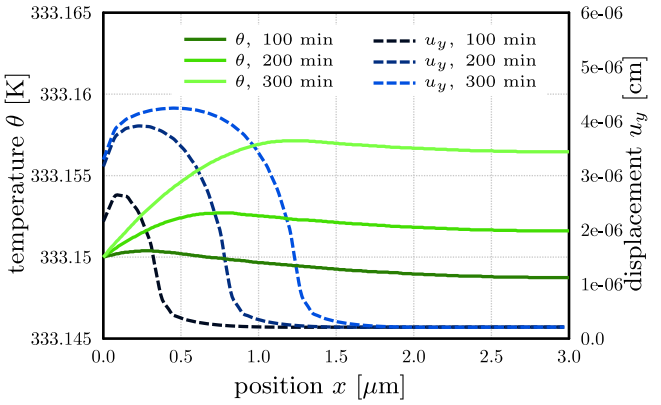

Fig. 7. Temperature and displacement profiles in x-direction of the undeformed sample at different exposure times. The expanded material cools due to the thermoelastic effect.

In Fig. 9, the equilibrium degree of swelling as a function of temperature is depicted. The volume of the swollen sample increases linearly with the increasing temperature. Thermal expansion only accounts for a minimal percentage of the volume increase.

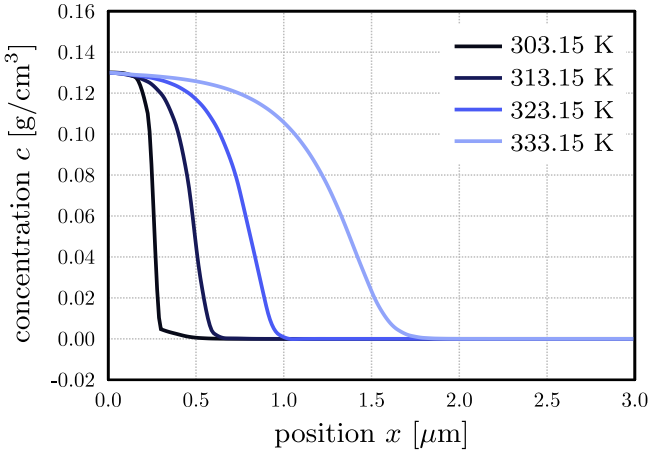

Fig. 8. Concentration profiles for different applied temperatures at an exposure time of $t = 300$ min. With increasing temperature, the diffusion becomes faster and the front broadens.

A pre-deformation of the specimen has only a very small influence on the modelled diffusion behaviour. However, from experiments, e.g., Harmon et al. (1987), it is known that a considerable pre-deformation causes a transition of the diffusion mechanism from Case II to Fickian behaviour. In its current form, the proposed model only considers the coupling between the deformation state and the diffusion coefficient. To account for the mechanism transition caused by pre-deformation, the model could be extended by a formulation for the generation of free volume during deformation and its influence on the diffusion kinetics.

4. Summary

A general framework for coupling diffusion and thermo-mechanics as proposed in Govindjee and Simo (1993), McBride et al. (2011a) has been adapted for the description of Case II diffusion. To this end, a formulation for the Helmholtz free energy of mixing has been derived from the Flory–Huggins theory of mixing. Furthermore, a quasi-hyperbolic diffusion law has been introduced to account for the characteristic kinetics of Case II diffusion. Here, a formulation for the diffusion coefficient has been applied that depends not only on concentration but also on the deformation state and the temperature.

During formulation of the governing equations and the simulations, special attention has been paid to the thermodynamical consistency of the model.

To examine the capacity of this model, it has been implemented in an in-house finite element code and used in numerical simulations of the diffusion of toluene in polystyrene. These numerical examples show that the model accurately describes the characteristic solvent uptake behaviour of Case II diffusion, namely the formation of a sharp diffusion front that moves with constant velocity as well as plasticisation and considerable swelling behind this front. The concentration and swelling reach their equilibrium values behind the front quickly, thus, displaying the characteristic step-like profiles.

Furthermore, the coupling to temperature allows to describe thermoelastic behaviour of the polymer as well as a change in the diffusion kinetics as the temperature approaches the glass transition temperature. Extension of this diffusion-temperature coupling is a promising approach for the description of non-Case II anomalous diffusion and the transition from Case II to Fickian behaviour.

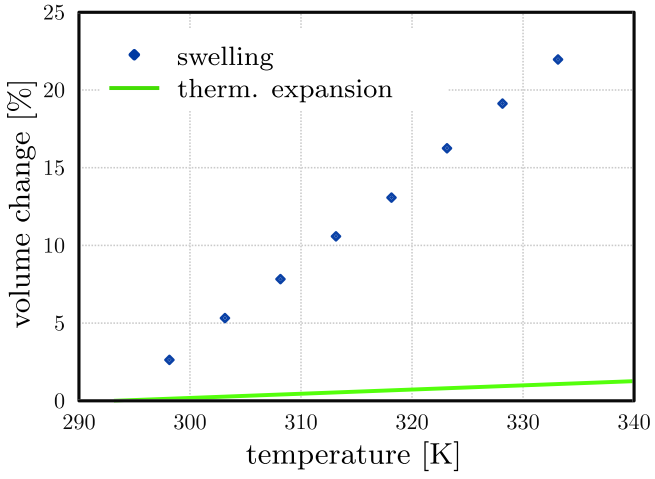

Fig. 9. Temperature dependence of the volume expansion. The equilibrium degree of swelling increases distinctly more with temperature than the thermal expansion does.

Appendix A. Further comments on thermodynamic relations

A.1. Chemical potential

As outlined in Section 2.2, the equation of state for the chemical potential is $\mu_s = \varphi_s - \theta\eta_s$. Furthermore, $\mu_s = \frac{\partial \Delta G^{\mathrm{mix}}}{\partial N_s} = \frac{\partial \Delta H^{\mathrm{mix}}}{\partial N_s} - \theta \frac{\partial \Delta S^{\mathrm{mix}}}{\partial N_s}$ holds. Therefore, the specific enthalpy φ_s and the specific entropy η_s contributions can be obtained from Eq. (21) and Eq. (18), respectively, according to

$$\varphi_s = \frac{\partial \Delta H^{\mathrm{mix}}}{\partial N_s} = \frac{k_{\mathrm{B}}\theta}{\rho_0 V}\frac{\chi}{J} \tag{A.1}$$

$$\begin{aligned}\eta_s &= \frac{\partial \Delta S^{\mathrm{mix}}}{\partial N_s} \\ &= -\frac{k_{\mathrm{B}}}{\rho_0 V}\left[\ln\frac{N_s}{N_s + rN_p} + \left[1-\frac{1}{r}\right]\frac{rN_p}{N_s + rN_p}\right] \\ &= -\frac{k_{\mathrm{B}}}{\rho_0 V}\left[\ln\frac{c_0}{c_0 + \rho_0\frac{m_s}{m_p}} + \left[1-\frac{1}{r}\right]\frac{\rho_0\frac{m_s}{m_p}}{c_0 + \rho_0\frac{m_s}{m_p}}\right].\end{aligned} \tag{A.2}$$

A.2. Evaluation of the reduced dissipation inequality

A thermodynamically consistent formulation needs to fulfil the reduced dissipation inequality which in its most general formulation is given in Eq. (13). For the considered constitutive relations without history variables $\boldsymbol{\Xi}$ and including the equation of state for the chemical potential, Eq. (13) reduces to

$$-\boldsymbol{J}\cdot[\nabla\varphi_s - \theta\nabla\eta_s] - \frac{1}{\theta}\boldsymbol{Q}\cdot\nabla\theta \geq 0. \tag{A.3}$$

As $\boldsymbol{Q} = -\boldsymbol{K}\cdot\nabla\theta$ with $\boldsymbol{K}$ being non-negative, the second term in Eq. (A.3) is always positive.

To account for the characteristic Case II kinetics, the diffusive flux is given by $\boldsymbol{J}(\boldsymbol{X},t+\tau_j) = -\boldsymbol{D}(c_0)\cdot\nabla c_0(\boldsymbol{X},t+\tau_c)$, cf. Section 2.2. With this relation, it is not obvious whether the term including the diffusion flux is greater or equal to zero. This is tested during simulations by calculating the dissipation density given by Eq. (A.3) in every quadrature point.

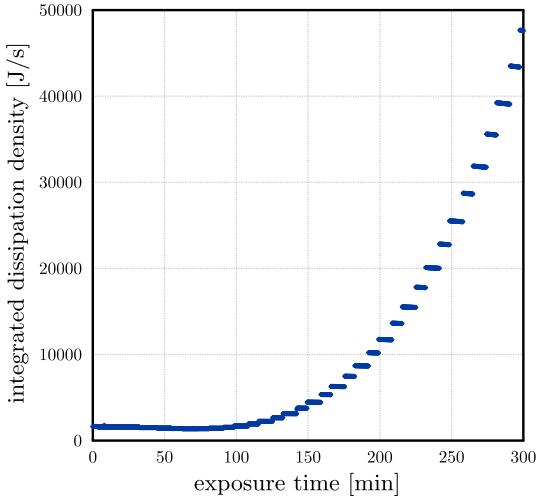

Fig. A.10. Dissipation of the whole system for the completely coupled case. As the dissipation density is positive in every time step, the dissipation inequality is fulfilled. The jumps in the curve are a product of the jump in the elasticity constants upon plasticisation.

The results for the completely coupled case with a boundary temperature of 333.15 K are given in Fig. A.10, which shows that the integrated dissipation density for the whole system is positive in every time step. This requirement is not only fulfilled for the whole system but in fact in every quadrature point.

References

Alfrey, T., Gurnee, E.F., Lloyd, W.G., 1966. Diffusion in glassy polymers. J. Polym. Sci. C Polym. Symp. 12 (1), 249–261.

Baek, S., Srinivasa, A.R., 2004. Diffusion of a fluid through an elastic solid undergoing large deformation. Int. J. Non-Linear Mech. 39 (2), 201–218.

Bangerth, W., Hartmann, R., Kanschat, G., 2007. deal.II – a general purpose object oriented finite element library. ACM Trans. Math. Softw. 33 (4), 24/1–24/27.

Bargmann, S., McBride, A.T., Steinmann, P., 2011. Models of solvent penetration in glassy polymers with an emphasis on Case II diffusion. A comparative review. Appl. Mech. Rev. 64 (1), 010803–1–010803–13.

Bouklas, N., Huang, R., 2012. Swelling kinetics of polymer gels: comparison of linear and nonlinear theories. Soft Matter 8, 8194–8203.

De Kee, D., Liu, Q., Hinestroza, J., 2005. Viscoelastic (non-fickian) diffusion. Can. J. Chem. Eng. 83 (6), 913–929.

Delassus, P.T., Whiteman, N.F., 1999. Physical and mechanical properties of some important polymers. In: Brandrup, J., Immergut, E.H., Grulke, E.A. (Eds.), Polymer Handbook, fourth ed. Wiley, New York, pp. V/159–V/169.

Derrien, K., Gilormini, P., 2006. Interaction between stress and diffusion in polymers. Defect Diffus. Forum 258–260, 447–452.

Duda, J.L., Vrentas, J.S., Ju, S.T., Liu, H.T., 1982. Prediction of diffusion coefficients for polymer-solvent systems. AIChE J. 28 (2), 279–285.

Durning, C.J., Tabor, M., 1986. Mutual diffusion in concentrated polymer solutions under a small driving force. Macromolecules 19 (8), 2220–2232.

Flory, P.J., 1942. Thermodynamics of high polymer solutions. J. Chem. Phys. 10, 51–61.

Flory, Paul J., 1970. Fifteenth spiers memorial lecture. Thermodynamics of polymer solutions. Discuss. Faraday Soc. 49, 7–29.

Fried, J., 2003. Conformation, Solutions, and Molecular Weight. book section 3. Pearson Education.

Gall, T.P., Kramer, E.J., 1991. Diffusion of deuterated toluene in polystyrene. Polymer 32 (2), 265–271.

Gallyamov, M.O., 2013. Sharp diffusion front in diffusion problem with change of state. Eur. Phys. J. E 36 (8), 1–13.

Govindjee, S., Simo, J.C., 1993. Coupled stress-diffusion: Case II. J. Mech. Phys. Solids 41 (5), 863–887.

Harmon, J.P., Lee, S., Li, J.C.M., 1987. Methanol transport in PMMA: the effect of mechanical deformation. J. Polym. Sci. A Polym. Chem. 25 (12), 3215–3229.

Holzapfel, G.A., 2000. Nonlinear Solid Mechanics, first ed. John Wiley & Sons.

Hong, W., Zhao, X., Zhou, J., Suo, Z., 2008. A theory of coupled diffusion and large deformation in polymeric gels. J. Mech. Phys. Solids 56 (5), 1779–1793.

Hopfenberg, H.B., Frisch, H.L., 1969. Transport of organic micromolecules in amorphous polymers. J. Polym. Sci. B Polym. Lett. 7 (6), 405–409.

Lasky, R.C., Kramer, E.J., Hui, C.-Y., 1988. Temperature dependence of Case II diffusion. Polymer 29 (6), 1131–1136.

Liu, S., Jiang, M., Ye, S., Xu, X., Lu, P., Dong, J., 2012. Biodegradable poly(glycerin citrate) and its application to controlled release of theophylline. J. Appl. Polym. Sci. 124 (5), 3633–3640.

Mark, J.E., Erman, B., 2007. Rubberlike Elasticity: a Molecular Primer. Cambridge University Press.

McBride, A.T., Bargmann, S., Steinmann, P., 2011a. Geometrically Nonlinear Continuum Thermomechanics Coupled to Diffusion: a Framework for Case II Diffusion. In: Volume 59 of Lecture Notes in Applied and Computational Mechanics. Springer, Berlin Heidelberg, pp. 89–107 book section 5.

McBride, A.T., Javili, A., Steinmann, P., Bargmann, S., 2011b. Geometrically nonlinear continuum thermomechanics with surface energies coupled to diffusion. J. Mech. Phys. Solids 59 (10), 2116–2133.

Schuld, N., Wolf, B.A., 1999. Polymer-solvent interaction parameter. In: Brandrup, J., Immergut, E.H., Grulke, E.A. (Eds.), Polymer Handbook, fourth ed. Wiley, New York.

Steinmann, P., McBride, A.T., Bargmann, S., Javili, A., 2012. A deformational and configurational framework for geometrically non-linear continuum thermomechanics coupled to diffusion. Int. J. Non Linear Mech. 47 (2), 13–13.

Vijalapura, P.K., Govindjee, S., 2003. Numerical simulation of coupled-stress Case II diffusion in one dimension. J. Polym. Sci. B Polym. Phys. 41 (18), 2091–2108.

Vijalapura, P.K., Govindjee, S., 2005. An adaptive hybrid time-stepping scheme for highly non-linear strongly coupled problems. Int. J. Numer. Methods Eng. 64 (6), 819–848.

Vrentas, J.S., Jarzebski, C.M., Duda, J.L., 1975. A Deborah number for diffusion in polymer-solvent systems. AIChE J. 21 (5), 894–901.

Wang, X., Hong, W., 2012. A visco-poroelastic theory for polymeric gels. Proc. R. Soc. A 468 (2148), 3824–3841.

Wilmers, J., Bargmann, S., 2014. Simulation of non-classical diffusion in polymers. Heat Mass Transf. 1–10.

Wu, J.C., Peppas, N.A., 1993. Modeling of penetrant diffusion in glassy polymers with an integral sorption Deborah number. J. Polym. Sci. B Polym. Phys. 31 (11), 1503–1518.